



## Short communication

## A novel core–shell nanocomposite electrolyte for low temperature fuel cells

Junsheng Wu<sup>a,b</sup>, Bin Zhu<sup>c</sup>, Youquan Mi<sup>c</sup>, Shao-Ju Shih<sup>d,f</sup>, Jun Wei<sup>e</sup>, Yizhong Huang<sup>b,f,\*</sup><sup>a</sup> Institute for Advanced Materials and Technology, University of Science and Technology Beijing, Beijing 100083, PR China<sup>b</sup> School of Materials Science and Engineering, Nanyang Technological University, Singapore 639798, Singapore<sup>c</sup> Department of Energy Technology, Royal Institute of Technology (KTH), Sweden<sup>d</sup> Department of Materials Science and Engineering, National Taiwan University of Science and Technology, Taipei 106, Taiwan<sup>e</sup> Singapore Institute of Manufacturing Technology, Singapore 638075, Singapore<sup>f</sup> Department of Materials, University of Oxford, Oxford, OX1 3PH, UK

## ARTICLE INFO

## Article history:

Received 29 July 2011

Received in revised form 5 October 2011

Accepted 24 October 2011

Available online 28 October 2011

## Keywords:

SDC core–shell nanocomposite

Electrolyte

Low temperature fuel cells

Ionic conductivity

## ABSTRACT

We report a rapid and cost-effective method to coat SDC nano-particles with a thin LiZn-oxide nanocomposite layer. This composite is determined to have a structure with two phases consisting of Li<sub>2</sub>O and ZnO and examined to distribute over the surfaces of SDC nano-particles uniformly by using energy dispersive X-ray (EDX) and high-resolution TEM (HRTEM). The measurements of electrical property demonstrate that such a thin layer enables the ionic conductivity of SDC to be significantly increased (higher than 0.1 S cm<sup>−1</sup> at the temperature of 300 °C) equivalent to the conductivity of pure SDC at 800 °C or YSZ at 1000 °C. This superionic conductivity is caused by the two-phase interfaces formed between nano-particles.

© 2011 Elsevier B.V. All rights reserved.

## 1. Introduction

Solid oxide fuel cells (SOFCs) are becoming an important and promising energy conversion technology in the 21st century. It has, however, been challenging to develop an electrolyte with superionic conductivity (i.e., conductivity  $\sigma \sim 10^{-2}$  S cm<sup>−1</sup> close to room temperature) for use in SOFCs [1,2]. Since ion conduction is caused by ion diffusion within the electrolyte, high temperature cases are normally required to increase ion mobility. A temperature in the range from 800 °C to 1000 °C, for instance, is required for zirconia (YSZ) or samarium-doped ceria (SDC) to achieve an ionic conductivity of 0.1 S cm<sup>−1</sup>. Most recently, development of SOFCs with superionic conductivity at the low temperature ranged between 300 °C and 600 °C has been of particular interest [2–8]. It is still far from manufacturing a satisfactory low temperature SOFC with a reasonably good performance due to the technical difficulty in designing and selecting a suitable functional material. YSZ thin film, for instance, is one of main candidates that has been studied in SOFCs and shows a great potential in the reduction of operational temperature [9–12]. However, as a consequence of their ionic conduction bulk mechanism imposed by a single-phase struc-

ture, these electrolytes are unlikely able to become the superionic conductors at low temperatures.

To yield a high performance of low temperature FCs, effort has been made by building new architectures using nanocomposites that allow two-phase interfaces to be produced resulting in an excellent conductivity. Such two-phase composites were at very early time developed by Uvarov et al. [13] based on the system of Li<sub>2</sub>SO<sub>4</sub> and Al<sub>2</sub>O<sub>3</sub> phases, which were separated by an intermediate thin layer of lithium aluminate produced by a strong interface interaction between two phases leading to an ionic conductivity comparable with that of superionic conductors.

This paper reports a novel functional nanocomposite we synthesized for the first time by using a simple and cost-effective method to coat a thin LiZn-oxide layer over the SDC nano-particles.

## 2. Experimental

## 2.1. Synthesis of SDC

SDC used as an electrolyte in SOFCs was synthesized by the solution route through co-precipitation. Firstly, 1 M aqueous solution cerium nitrate (supplied by Sigma–Aldrich) and 1 M aqueous solution samarium (III) nitrate (Aldrich) were prepared separately. Two solutions were then mixed at a certain molar ratio. The sodium carbonate (Sigma–Aldrich), served as a precipitation agent with a molar ratio of Ce<sup>3+</sup>/Sm<sup>3+</sup>:CO<sub>3</sub><sup>2−</sup> = 1:1.5, was subsequently added into the mixed Ce<sup>3+</sup>/Sm<sup>3+</sup> solution forming the SDC precursor. The

\* Corresponding author at: School of Materials Science and Engineering, Nanyang Technological University, Singapore 639798, Singapore.

E-mail addresses: [yzhuang@ntu.edu.sg](mailto:yzhuang@ntu.edu.sg), [yizhong.huang@materials.ox.ac.uk](mailto:yizhong.huang@materials.ox.ac.uk) (Y. Huang).

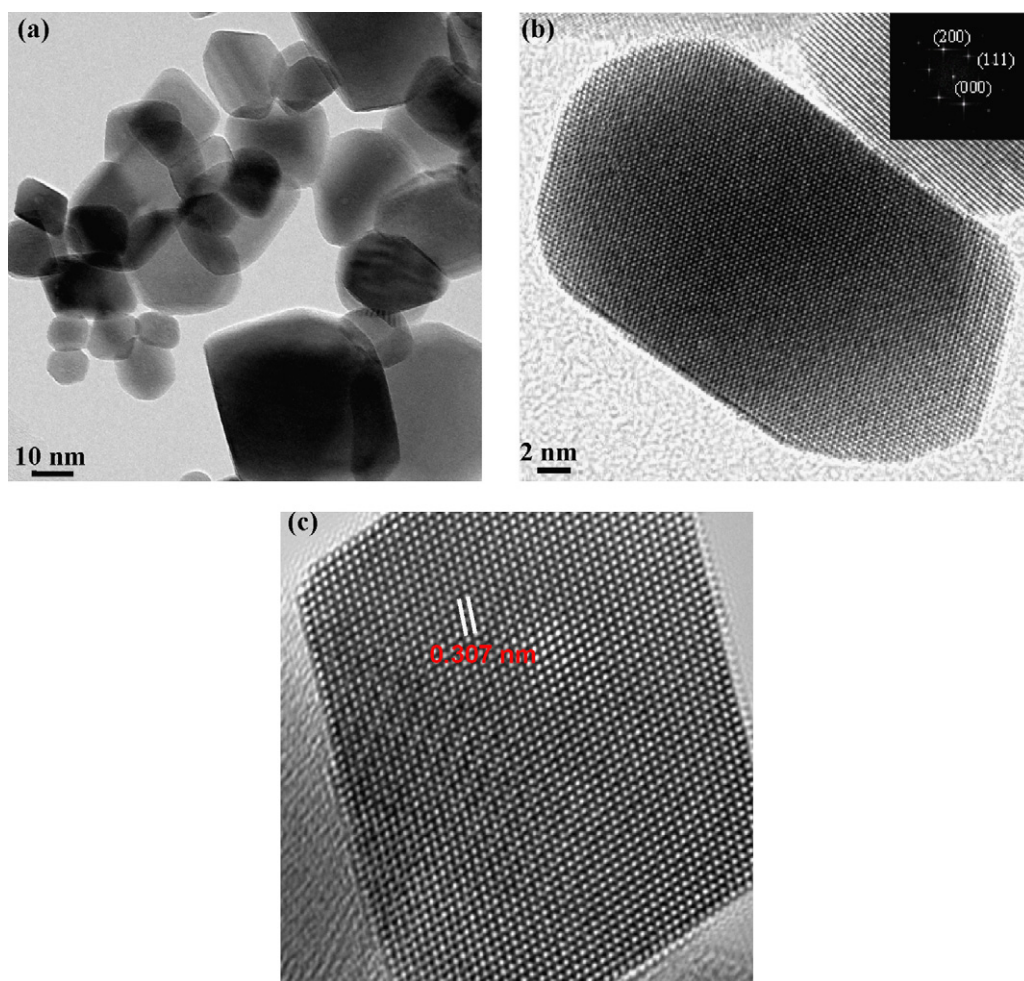


**Fig. 1.** (a) A bright-field TEM image where a number of SDC nano-particles are visible with a wide range of sizes; (b) a high-resolution TEM image of a SDC nanoparticle showing its perfection of crystalline structure; (c) atomic image of a SDC nanoparticle.

pH value of the solution was adjusted to 12 by adding sodium hydroxide. The obtained precipitate was rinsed several times with deionized water followed by washing up thoroughly using ethanol to remove the water from the particle surfaces. The precipitate was then dried in an oven at 100 °C overnight and finally ground into powder before sintered at 700 °C for 2 h.

## 2.2. Synthesis of core-shell nanocomposite

$\text{LiNO}_3$  and  $\text{Zn}(\text{NO}_3)_2 \cdot \text{H}_2\text{O}$  (Sigma-Aldrich) with a molar ratio of 1 Li:1 Zn were mixed and prepared into a 1 M aqueous solution. Citric acid with amount (mol) being 1.5 times more than that of  $\text{LiNO}_3$  or  $\text{Zn}(\text{NO}_3)_2$  (mole) was then added into the Li–Zn solution, which was subsequently heated up to 120 °C and stirred sufficiently forming a sol–gel solution. After that, the same amount of SDC powder (mol) was added into above Li–Zn sol–gel solution while stirring until a dense gel mixture was produced. The mixture was stored in an oven at a temperature of 120 °C for overnight so that a dried puff gel was formed. SDC powder coated with LiZn-oxide was ultimately obtained after the dried gel was sintered at 700 °C for 2 h.

## 2.3. Microstructural characterization of nano-particles

Microstructural characterization of as-prepared samples was performed using high-resolution transmission electron microscopes, JEOL 3000F TEM and JEOL 2200FS TEM with an objective

Cs-corrector operated at 300 keV and 200 keV, respectively. Elemental mapping was implemented by energy dispersive X-ray (EDX) technique in the scanning TEM mode with an Oxford Instruments INCA Energy X-ray detector attached to the JEOL 3000F TEM.

## 2.4. Solid state fuel cell fabrication

The fuel cell was manufactured using LiZn-oxide coated SDC electrolyte. It consists of an anode (NiO mixed with the electrolyte) and a cathode (a mixture of lithiated NiO and the electrolyte). The anode, LiZn-oxide coated SDC nanocomposite and the cathode with a volume ratio between the electrolyte and the electrodes of 1 were uniaxially pressed at 250 MPa forming a sandwich structure through a hot pressing process at 550 °C in one successive step. This step involves loading powder mold in a particular order from anode, then electrolyte until cathode. The fuel cell has a diameter 13 mm (with a 0.7 cm<sup>2</sup> active area) with a total thickness of around 1.0 mm in which the electrolyte layer is 0.4 mm thick and two electrodes have same thickness, i.e., 0.3 mm each. Finally, silver paste, acted as current collector during fuel cell measurements, was painted on the surfaces of both anode and cathode. The cell was tested at 420–520 °C in which hydrogen and air were used as fuel and oxidant, respectively. The gas flow rates were controlled in the range of 80–120 ml min<sup>−1</sup> at 1 atm pressure.

### 2.5. Property measurements

The electrical properties were measured using AC impedance analysis in the frequency range between 5 Hz and 13 MHz using a computerised HP 4192A LF Impedance Analyzer with an applied signal of 20 mV. The temperature of the sample holder was controlled by a Eutherm temperature controller and the sample temperature was monitored by a Platinum thermocouple attached to the sample. The measurements were carried out between 300 °C and 600 °C in air.

The fuel cell was measured under variable resistance loads, which adjust the outputs of cell voltage and power. By collecting data of the cell voltage and current at each resistance load, a series of  $I$  (current)– $V$  (voltage) or  $I$ – $P$  (power) curves can be plotted. Data collection and processing were implemented with the aid of a computer.

### 3. Results and discussion

Fig. 1(a), a bright-field TEM image, shows the SDC particles with the sizes less than 100 nm. The shapes of the nano-particles are found to be dependent of their dimensions. They appear spherical when they are very small (approximately 10 nm) but show quadrangular shape at relatively large size. The perfection of their crystalline structures was viewed in TEM. As an example, Fig. 1(b) shows a high-resolution TEM (HRTEM) image of a pure SDC particle. A face-centered cubic structure is determined by analyzing the fourier transfer function (inset in Fig. 1(b)). Fig. 1(c) is also an HRTEM image of another SDC particle, which shows a perfect atomic arrangement. The  $d$ -spacing of the (111) plane is measured to be 0.307 nm, which is in good agreement with the (111)  $d$ -spacing observed for SDC from XRD (0.308 nm measured from Fig. 2). These measured  $d$ -spacings are slightly less than that of pure ceria (0.314 nm). This is due to the substitution of Sm atoms in Ce lattice sites. Since Sm has a slightly smaller atomic volume than Ce, the replacement of Sm at the lattice positions of Ce results in a contraction of the lattice structure.

The SDC nano-particles coated with LiZn-oxide were also observed in TEM. Fig. 3(a) shows a bright-field TEM image, where

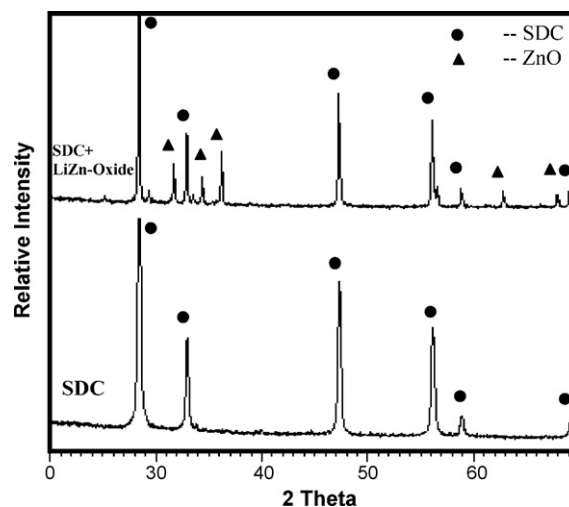


Fig. 2. Two XRD spectra collected from pure SDC and coated SDC.

the nano-particles were chemically mapped by EDX. Elemental distributions were obtained and are shown in Fig. 3(b–e), corresponding to elements Ce, Sm, Zn and O, respectively. It is reasonable to see elements Sm, Ce and O as they are the contents of the nano-particles. However, as to be expected, element Zn is detected and uniformly distributed over the surfaces of the SDC nano-particles as shown in Fig. 3(d) (Li is too light to be detected by EDX). This suggests that the LiZn-oxide has been successfully coated on to the nano-particles, which is further confirmed by an HRTEM image (Fig. 4(a)). The adjacent lattice fringes of LiZn-oxide coating layer are measured to be approximately 0.267 nm corresponding to the  $d$ -spacing of (401) plane of LiZn-oxide, which is consistent with the XRD measurement from Fig. 2 and a simulated HRTEM image (Fig. 4(b)).

The conductivities of uncoated SDC, LiZn-oxide coated SDC and  $1/2\text{Li}_2\text{O}-\text{ZnO}$  as a function of temperature were measured and results are shown in Fig. 5, where a very high conductivity up to  $0.1\text{ S cm}^{-1}$  for LiZn-oxide coated SDC at about 400 °C is demon-

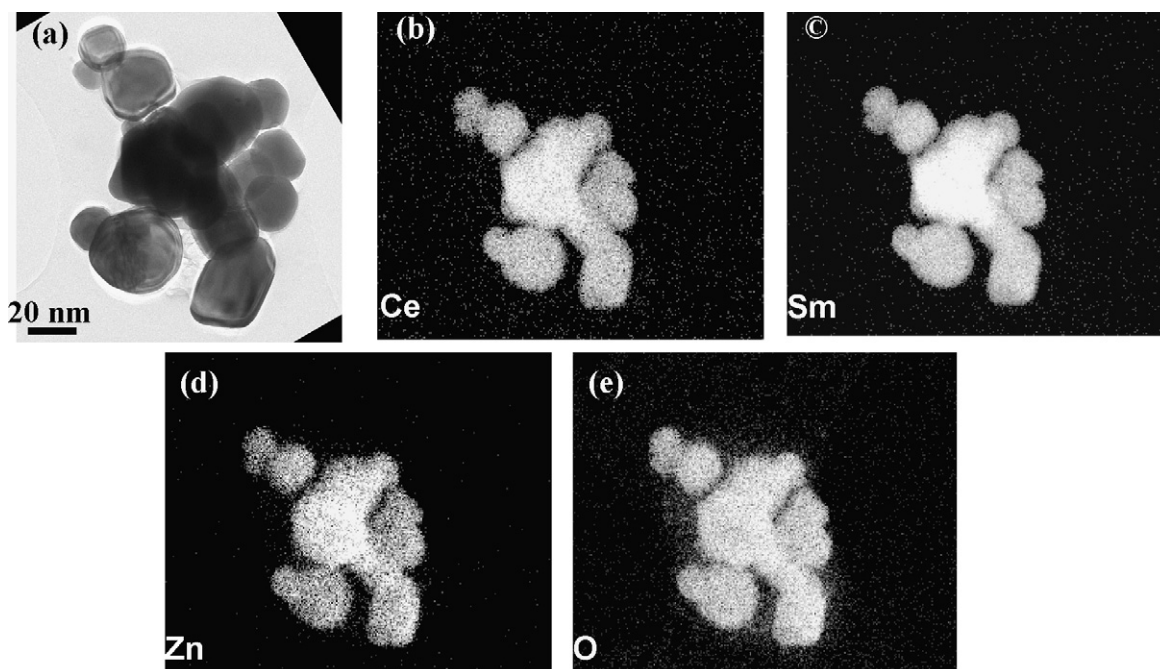
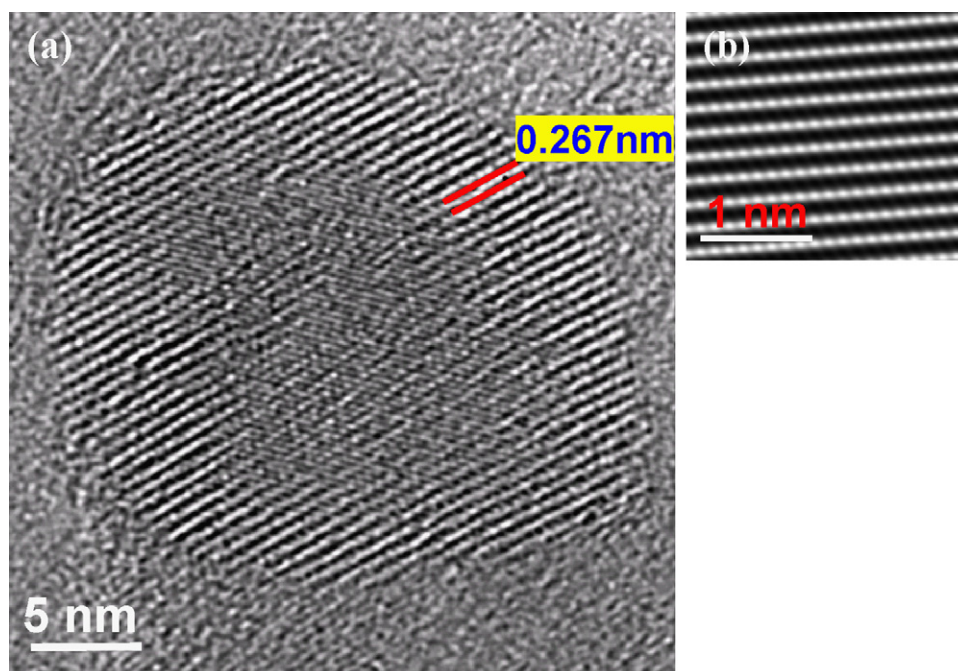


Fig. 3. (a) A bright-field TEM image where elemental mapping was carried out; (b–e), chemical images for elements Ce, Sm, Zn and O.





**Fig. 4.** (a) A high-resolution TEM image showing a core-shell structure of a SDC nanoparticle which is covered by a thin layer of LiZn-oxide; (b) simulated HRTEM image of ZnO coating at [2 1 0] projection.

strated. It is significantly higher than the conductivities of both uncoated SDC electrolyte and LiZn-oxide and as good as the conductivity of the conventional SOFC electrolytes, YSZ at 1000 °C and SDC at 800 °C. It is worth to note that the presence of a peak at 420 °C in the curve of the LiZn-oxide in Fig. 4 is apparently due to phase transition [14]. This result is in good agreement with the investigation from Tsukamoto et al. He suggested that  $1/2\text{Li}_2\text{O}-\text{ZnO}$  has a hexagonal structure with the cell parameters  $a = 0.812$  nm and  $c = 0.673$  nm. Electrical conductivity increased with increasing temperature up to 420 °C, and decreased abruptly above 420 °C. This temperature dependence of the ionic transference number confirmed that ionic conduction dominates above 300 °C, while mixed conduction (i.e., ionic conduction and electrical conduction) occurs below 300 °C [15].

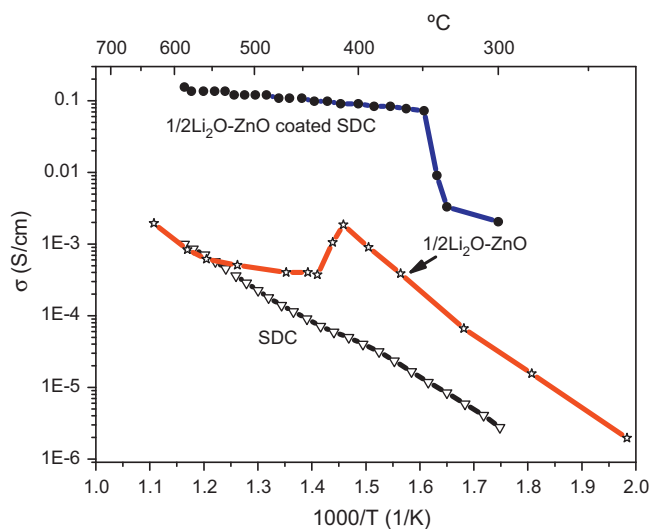


**Fig. 5.** The dependence of conductivity of non-coated SDC and LiZn-oxide coated SDC on temperature in comparison with the conductivity curve of  $1/2\text{Li}_2\text{O}-\text{ZnO}$  cited from literature reported by Tsukamoto et al.

In principle, ionic conductivity relies on the pre-exponential factor  $\sigma_0$  and the ionic migration activation energy  $E_a$  as illustrated in the Arrhenius equation:  $\sigma T = \sigma_0 \exp(-E_a/kT)$ , where  $k$  is Boltzmann constant and  $T$  temperature. At constant temperature, increasing the pre-exponential factor, which is proportional to mobile ion concentration ( $n$ ) and ion jump-step distance ( $d$ ), or decreasing activation energy will result in an increase of ionic conductivity. Due to a strong interaction between vacancies and cations, the materials with a single-phase, such as YSZ and SDC, usually show an  $E_a$  (around 1.0 eV) much higher than superionic conduction activation energy (for superionic conductors where the ionic conductivity is more than  $10^{-1} \text{ S m}^{-1}$  at 300 K and activation energy for ion transport is approximately 0.1 eV). On the other hand, a single-phase crystalline structure turns out a very low  $\sigma_0$ . This is because it has a small ion concentration, which is imposed by the degree of doping, resulting in a low concentration of extrinsically created vacancies, e.g., 10 mol% of Y in YSZ and a small ion jump distance in the unit cell. These demonstrate that the vacancy mechanism or the bulk effect in the crystalline structure with a single-phase brings about high activation energy and a small oxygen ion mobility and concentration leading to a low ionic conductivity. To increase it, a sufficient high temperature is required.

To achieve low temperature (between 300 °C and 600 °C) SOFCs, new functional electrolyte materials are needed and should not be subject to above limits. The current work presents a newly developed core-shell structure. The two-phase interfaces within this novel structure form an ionic highway network allowing oxygen ions having a superionic conduction in the electrolyte [16].

In LiZn-oxide coated SDC nanocomposite, the nano-particles are separated by the thin conducting LiZn-oxide coating. Zn-oxide is a typical n-type semiconductor and can react with  $\text{Li}_2\text{O}$ . In the present work, LiZn-oxide had a mole ratio of 1 Li:1 Zn and the resulting coating LiZn-oxide is likely a mixture of  $1/2\text{Li}_2\text{O}-\text{ZnO}$ , as proved by XRD spectra (Fig. 2).

A case study has been made on the basis of ceria-carbonate two-phase materials to discuss interfacial ion interaction, the interface electric field and the corresponding oxygen ion activation energy [16]. A simple Coulombic model is used to illustrate the interactions

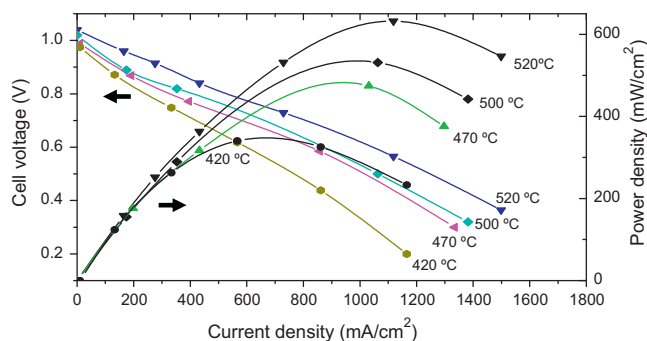


**Fig. 6.** *I*-*V* and *I*-*P* characteristics of a single cell prepared using the coated SDC nanocomposite as an electrolyte operated at various temperatures.

in the interface region. A special attention is paid to the Coulombic interactions between the oxygen ions on the ceria particle and  $M^+$  ( $Li^+$ ,  $Na^+$  or  $K^+$ ) cations. Since an electrical field is established in the interfaces between two constituent phase particles, the migration activation energy, i.e., the oxygen ion mobility has to overcome this Coulombic potential. With a distance of 10 nm for the interfacial region, the oxygen ion activation energy less than 0.2 eV is obtained, which is reasonably low for oxygen ion transport. The same model can be applied to the LiZn-oxide and SDC two-phase system, where  $Li^+/Zn^{2+}-O^{2-}$  interactions may result in the similar activation energy. More importantly, a great number of defects (such as dislocation) formed in the interface between SDC and LiZn-oxide due to lattice mismatch (see Fig. 3) allow the transport of  $O^{2-}$  ions within electrolyte at a much low activation energy leading to the possible superionic conduction above 300 °C.

Fig. 6 shows the electrical performance of a SOFC fabricated using the LiZn-oxide coated SDC as electrolyte. Apparently, the cell voltage drops and the higher resistance loaded causes it dropping more rapidly. The open circuit voltages (OCV) are almost 1.0 V, indicating that these composite electrolytes can form a relative gas tight electrolyte membrane to avoid gas crossover. The maximum power density of  $630 \text{ mW cm}^{-2}$  has been achieved at 520 °C, which is  $545 \text{ mW cm}^{-2}$  at 600 °C for the uncoated SDC [17]. This significant enhancement is apparently attributed to the high ionic conductivity of the coated SDC nanocomposite. Therefore, we believe that by taking advantage of this coated SDC nanocomposite we are able to make immediate success in development of low temperature SOFCs.

The interfacial mechanism and material two-phase architecture display a new scientific principle in material design and development. This is significantly different from the single-phase materials such as YSZ and SDC. The conventional ionic doping and bulk mechanism requires high temperatures to activate ionic mobility. Manipulation of interphases of nanotech-based composites of ceria two-phase materials can tremendously reduce the working temperature of the SOFC from 1000 °C to 300–600 °C

which opens a new technological opportunity for the future energy production.

#### 4. Summary

In this paper, the LiZn-oxide has been successfully coated on SDC nano-particles (less than 100 nm in size) forming a two-phase nanocomposite thin film, which is distributed over the surfaces of SDC nano-particles uniformly, as proved by EDX and HRTEM. Electrical property measurements show that such a thin layer has significantly enhanced ionic conductivity, which reaches higher than  $0.1 \text{ S cm}^{-1}$  at the temperature of 300 °C equivalent to the pure SDC at 800 °C or YSZ at 1000 °C. This enhancement of conductivity is benefited from the interfaces between nano-particles which is unable to achieve from conventional single-phase bulk materials. These new materials based on the novel core-shell LiZn-oxide coated SDC nanocomposites have opened a new advanced 300–600 °C SOFC technology and is likely to make a breakthrough in SOFC materials and technology.

#### Acknowledgements

Authors thank the financial support from the Swedish Research Council and the Swedish Agency for International Development Cooperation (SIDA) and the EC FP6 NANOCOFC project (contract no. 032308). Discussion with Professor Joost Vlassak is gratefully acknowledged.

#### References

- [1] B.C.H. Steele, A. Heinzel, *Nature* 414 (2001) 345.
- [2] J.B. Goodenough, *Nature* 404 (1999) 821.
- [3] T. Hibino, A. Hashimoto, T. Inoue, J.I. Tokuno, S.I. Yoshida, M. Sano, *Science* 288 (2000) 2031.
- [4] E.P. Murray, T. Tsai, S.A. Barnett, *Nature* 400 (1999) 649.
- [5] S. Park, J.M. Vohs, R.J. Gorte, *Nature* 404 (2000) 265.
- [6] Z.G. Tang, Q.Z. Lin, B.E. Mellander, B. Zhu, *International Journal of Hydrogen Energy* 35 (2010) 2970.
- [7] J. Di, M.M. Chen, C.Y. Wang, J.M. Zheng, L.D. Fan, B. Zhu, *Journal of Power Sources* 195 (2010) 4695.
- [8] L.D. Fan, C.Y. Wang, M.M. Chen, J. Di, J.M. Zheng, B. Zhu, *International Journal of Hydrogen Energy* 36 (2011) 9987.
- [9] P. Charpentier, P. Fragnaud, D.M. Schleich, E. Gehain, *Solid State Ionics* 135 (2000) 373.
- [10] Z.P. Shao, M.H. Sossina, *Nature* 49 (2004) 170.
- [11] H. Huang, M. Nakamura, P. Su, R. Fasching, Y. Saito, F.B. Prinz, *Journal of the Electrochemical Society* 154 (2007) B20.
- [12] Y.I. Park, P.C. Su, S.W. Cha, Y. Saito, F.B. Prinz, *Journal of the Electrochemical Society* 153 (2006) A431.
- [13] N.F. Uvarov, B.B. Bokhonov, V.P. Isupov, E.F. Hairtdinov, *Solid State Ionics* 74 (1994) 15–27.
- [14] R.M. Biefeld, R.T. Johnson, *Journal of the Electrochemical Society* 126 (1979) 1.
- [15] Tsukamoto, C. Yamagishi, K. Koumoto, H. Yanagida, *Journal of Materials Science* 19 (1984) 2493.
- [16] B. Zhu, S. Li, B.-E. Mellander, *Electrochemistry Communications* 10 (2008) 302–305.
- [17] X. Zhang, M. Robertson, C. Deces-Petit, W. Qu, O. Kesler, R. Maric, D. Ghosh, *Journal of Power Sources* 164 (2007) 668.